



Energy-Exergetic performance and parametric evaluation of Haylent liquefaction system using different gasses system

R.S. Mishra, Devender Kumar

Department of Mechanical, Production and Automobile Engineering, Delhi Technological University, Delhi, India

Abstract

The present studies concern on energy and exergy analyses of various cryogenics system up to their sub component level. A parametric study is conducted to investigate the effects of variation of various system input parameters such as pressure ratio, expander mass flow ratio, compressor output temperature on different performance parameters like COP, work input, liquefaction rate, specific heat and exergy. The numerical computations have been carried out for six system are study with six different gases for liquefaction like oxygen, argon, methane, fluorine, air and nitrogen respectively. Effect of different input gas also studies carefully and behavior of different gases in different system is concluded.

© 2017 ijrei.com. All rights reserved

Keywords: Energy-Exergetic Performance, Parametric Evaluation, Haylent liquefaction system

1. Introduction

Cryogenics has been an important area of refrigeration because of its application in industrial and commercial utilization, and many scientific and engineering researches are going on by using low temperature liquefied gases. Cryogenics is a branch of physics which deals with the achieving very low temperatures (below the 173 K.) and study their effects on matter. Cryogenic study presents broad goals for cryogenic support for various gas liquefaction systems. Due to industrial revolution, various issues like cost, efficiency and reliability are the challenges factors in employment of cryogenic support technology. In field of mechanical engineering we try to refine or improve the ability or quality of material to get in maximum use at maximum level at a reduce cost. In past many fantastic claims have been made as to the degree of improve performance achieved by employing cryogenics technology. In 1949 Helandt Davies in his research noticed that if the Claude system work on relative high pressure, e.g., approx. 200 bar for air liquefaction. The first heat exchanger in the system can eliminate; such modified system is extensively used in high-pressure liquefaction plant of air and known as high pressure modified Claude system or Haylent system. The

problem of lubrication in expander is successfully eliminated in this modification. Use of light lubricant are quite suitable because, in the air-liquefaction system, the gas enters the expander at ambient temperature and leaves the expander at approximately 150 K (-190°F), so that light lubricants properties not much detroit. In high pressure Haylent system expander adjustment is also very crucial. All sub-component like compressor, expander, two heat exchangers with throttle valve and separator are arranged as shown in Figure .1. The block diagram completely define the working of system. The gas which has to be liquefied is fed in compressor at ambient condition like at 1.013 bar and 300 K. The gas is compressed up to their optimized pressure ratio selected on the basis of chosen gas. This compressed gas is further divided in two parts in perfect ratio for expander. One part of gas goes into expander while other part fed into the heat exchanger as a hot stream. Expander gives additional refrigeration effect in the system by giving additional cooling effect to the cold stream of gas into exchanger. After passing through the heat exchanger gas reached up to their critical temperature.

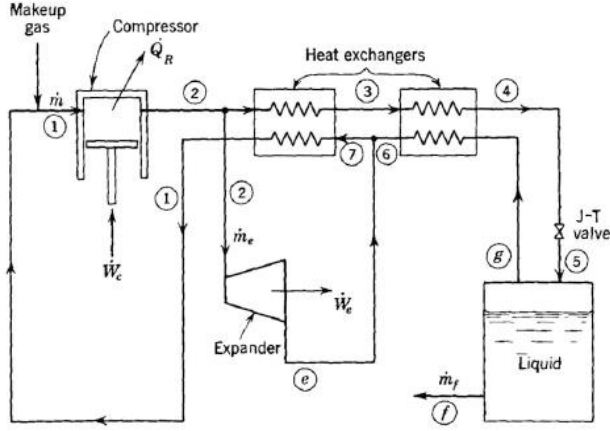


Figure 1: Schematic diagram of Haylent system

Now gas is passed through the J-T valve to get liquefy form of gas at the inlet pressure. The liquefy part is separate into the separator and gas part is recirculated back to the system via mixing with outlet of expander cooled gas. This mixed gas help into the exchanger to reduce the gas temperature up to their critical level via exchanging heat with hot stream. This cold stream after exchanging heat with hot stream add up with make gas to go again in cycle. The main difference in refrigeration and liquefier is that in refrigeration cycle the gas of system always constant while in liquefier the gas is continuously extracted as a liquefy part.

2. Literature Review and Research gap identified

R. Agrawal, D.W. Woodward,[1] carried out exergy analysis, for the efficient cryogenic nitrogen generators: Yasuki Kansha, et.al [2] , evaluated novel cryogenic air separation process based on self-heat recuperation. Gadhiraaju Venkatarathnam [3], carried out simulation of cryogenic processes” using cryogenic mixed refrigeration Processes. R.L. Cornelissen, G.G. Hirs,[4] carried out energy-exergy analysis of cryogenic air separation, There is not enough literature available on second law performance on Haylent system. The thermodynamic analysis of Haylent system is presented here.

3. Thermal analysis of Haylent system

The work done by the compressor is given as

$$W_e = (m_e * h_2 - m_e * h_e) \quad (1)$$

$$W_c = (m * ((h_2 - h_1) - T_2 * (s_2 - s_1))) \quad (2)$$

$$W_{net} = W_c - W_e \quad (3)$$

$$Q = m * (h_2 - h_1) \quad (4)$$

$$y = \left(\frac{h_1 - h_2}{h_1 - h_f} \right) + r * \left(\frac{h_2 - h_e}{h_1 - h_f} \right) \quad (5)$$

$$y = \frac{m_f}{m} \quad (6)$$

$$Ed_{comp} = abs \left(\left(m * T_1 * (s_1 - s_2) - \left(Q * \left(\frac{T_0}{T_1} \right) \right) \right) \right) \quad (7)$$

$$Ed_{comp\%} = \left(\frac{Ed_{comp}}{Ed_{Haylent}} \right) * 100 \quad (8)$$

$$x_f = 0 \quad (9)$$

$$x_g = 1 \quad (10)$$

$$r = 0.3 \quad (11)$$

$$r = \frac{m_e}{m} \quad (12)$$

$$\frac{W_{net}}{m} = z \quad (13)$$

$$\frac{W_{net}}{m_f} = t \quad (14)$$

$$COP = abs \left(\frac{h_1 - h_f}{W_{net}} \right) \quad (15)$$

$$Eta_{2nd\%} = abs \left(\left(\frac{(h_f - h_1) - T_0 * (s_f - s_1)}{W_{net}} \right) * m_f \right) * 100 \quad (16)$$

2.1 First Heat Exchanger (HX_1) analysis

TypeHX₁\$ = ' counterflow'

$$epsilon_{HX1} = 0.85 \quad (17)$$

$$T_{hi} = T_2 \quad (18)$$

$$T_{co} = T_8 \quad (19)$$

$$T_{ho} = T_3 \quad (20)$$

$$T_{ci} = T_7 \quad (21)$$

$$m_{dot_{hHX1}} = m - m_e \quad (22)$$

$$m_{dot_{cHX1}} = m - m_f \quad (23)$$

$$C_{dot_{hHX1}} = m_{hHX1} * cp_{hotfluidHX1} \quad (24)$$

$$C_{dot_{cHX1}} = m_{cHX1} * cp_{coldfluidHX1} \quad (25)$$

$$q_{HX1} = C_{hHX1} * (T_{hi} - T_{ho}) \quad (26)$$

$$q_{HX1} = C_{cHX1} * (T_{co} - T_{ci}) \quad (27)$$

$$q_{maxHX1} = C_{minHX1} * (T_{hi} - T_{ci}) \quad (28)$$

$$epsilon_{HX1} = \frac{q_{HX1}}{q_{maxHX1}} \quad (29)$$

$$Ntu_{HX1} = \frac{G_{HX1}}{C_{minHX1}} \quad (30)$$

$$Ex_{inHX1} = (m - m_e) * ((h_2 - h_3) - (T_0 * (s_2 - s_3))) \quad (31)$$

$$Ex_{outHX1} = (m - m_f) * ((h_7 - h_8) - (T_0 * (s_7 - s_8))) \quad (32)$$

$$Ed_{HX1} = abs((Ex_{inHX1}) - (Ex_{outHX1})) \quad (33)$$

$$Ed_{HX1\%} = \left(\frac{Ed_{HX1}}{Ed_{Haylent}} \right) * 100 \quad (34)$$

$$T_6 = T_7 \quad (35)$$

$$T_6 = T_7 \quad (35)$$

$$T_6 = T_7 \quad (35)$$

$$T_6 = T_7 \quad (35)$$

$$T_6 = T_7 \quad (35)$$

$$T_6 = T_7 \quad (35)$$

$$T_6 = T_7 \quad (35)$$

$$T_6 = T_7 \quad (35)$$

$$T_6 = T_7 \quad (35)$$

$$T_6 = T_7 \quad (35)$$

$$T_6 = T_7 \quad (35)$$

$$T_6 = T_7 \quad (35)$$

$$T_6 = T_7 \quad (35)$$

$$T_6 = T_7 \quad (35)$$

$$T_6 = T_7 \quad (35)$$

$$q_{\max HX2} = C_{\min HX2} * (T_3 - T_g) \quad (43)$$

$$\epsilon_{HX2} = \frac{q_{HX2}}{q_{\max HX2}} \quad (44)$$

$$Ntu_{HX2} = (G_{HX2})/C_{\min HX2} \quad (45)$$

$$Ex_{inHX2} = (m - m_e) * ((h_3 - h_4) - (T_0 * (s_3 - s_4))) \quad (46)$$

$$Ex_{outHX2} = (m - m_f) * ((h_g - h_6) - (T_0 * (s_g - s_6))) \quad (47)$$

$$Ed_{HX2} = \text{abs}((Ex_{inHX2}) - (Ex_{outHX2})) \quad (48)$$

$$Ed_{HX2\%} = \left(\frac{Ed_{HX2}}{Ed_{Haylent}}\right) * 100 \quad (49)$$

"c) J-T Valve analysis"

$$h_4 = h_5 \quad (50)$$

$$Ex_{inval} = (h_4 - h_0) - T_0 * (s_4 - s_0) \quad (51)$$

$$Ex_{outval} = (h_5 - h_0) - T_0 * (s_5 - s_0) \quad (51)$$

$$Ed_{val} = \text{abs}(Ex_{inval} - Ex_{outval}) \quad (52)$$

$$Ed_{val\%} = \left(\frac{Ed_{val}}{Ed_{Haylent}}\right) * 100 \quad (53)$$

"c) Seperator analysis"

$$(m - m_e) * h_5 = m_f * h_f + (m - m_e - m_f) * h_g \quad (54)$$

$$Ed_{sep} = \text{abs}\left(T_0 * \left(\left(\frac{m_g * s_{g1}}{(m_g + m_f) * s_5}\right) + \left(\frac{m_g * h_g - m_f * h_f}{T_0}\right)\right)\right) \quad (55)$$

$$Ed_{sep\%} = \left(\frac{Ed_{sep}}{Ed_{Haylent}}\right) * 100 \quad (56)$$

$$m_g = (m - m_e - m_f) \quad (57)$$

$$s_{g1} = \text{entropy}(R\$, h = h_g, P = P_1) \quad (58)$$

$$Ed_{Haylent} = Ed_{comp} + Ed_{HX1} + Ed_{HX2} + Ed_{val} + Ed_{sep} \quad (59)$$

$$Ntu_{HX1} = HX(\text{TypeHX1}\$, \epsilon_{HX1}, C_{hHX1}, C_{cHX1}, 'Ntu') \quad (60)$$

$$Ntu_{HX2} = HX(\text{TypeHX2}\$, \epsilon_{HX2}, C_{hHX2}, C_{cHX2}, 'Ntu') \quad (61)$$

In Non ideal gas any variable can be defined by two other dependent variable on them:

$$a_{\text{non-ideal gas}} = f(x(b, c))$$

Table 1: Variable Table (Heylant System)

Variable (a)	Gas	Variable (b)	Variable (c)
h_0	R\$	T_0	P_1
h_1	R\$	T_1	P_1
h_2	R\$	T_2	P_2
s_0	R\$	T_0	P_1
s_1	R\$	T_1	P_1
s_2	R\$	h_2	P_2
T_e	R\$	s_2	P_1
h_e	R\$	T_1	P_1
s_f	R\$	x_f	P_1
T_f	R\$	x_0	P_1
h_f	R\$	x_f	P_1

T_g	R\$	x_1	P_1
s_g	R\$	x_1	P_1
T_3	R\$	h_3	P_2
s_3	R\$	T_3	P_2
h_3	R\$	T_3	P_2
$cp(hf)_{HX1}$	R\$	T_2	P_2
$cp(cf)_{HX1}$	R\$	T_7	P_1
C_{\min}	-	C_{hot_HX1}	C_{cold_HX1}
$cp(hf)_{HX2}$	R\$	T_3	P_2
$cp(cf)_{HX2}$	R\$	$T_f - 1$	P_1
C_{\min}	-	C_{hot_HX2}	C_{cold_HX2}
h_7	R\$	T_7	P_1
s_7	R\$	T_7	P_1
h_8	R\$	T_8	P_1
s_8	R\$	T_8	P_1
s_5	R\$	h_5	T_f
s_4	R\$	h_4	T_4
h_4	R\$	T_4	P_2
s_{g1}	R\$	h_g	P_1
s_5	R\$	x_5	P_1
h_6	R\$	x_6	P_1
s_6	R\$	T_6	P_1
h_6	R\$	T_6	P_1

4. Results and Discussions

In this study, Haylent system for liquefaction of various gases such as oxygen, nitrogen, argon, methane, fluorine and air are studied. Fig.2 shows the variations between COP of the system and the cycle pressure ratio. It has been seen that COP is decreasing with an increase in cycle pressure ratio and methane has the highest value of COP, which is decreasing from 1.662 to 1.244 between pressure ratio 40 to 220, followed by fluorine, oxygen, air, nitrogen and argon has the least value of COP, i.e., varies from 0.8802 to 1.247 for the cycle pressure ratio of 40 to 220. On the other hand, fig-2 shows the variations in second law efficiency with respect to cycle pressure ratio. It has been demonstrated that methane has the highest value of second law efficiency, which is increasing from 5.792% to 21.23% for the cycle pressure ratio of 40 to 220, followed by argon, oxygen, air, nitrogen and fluorine has the minimum value of second law efficiency i.e., changes from 2.889% to 9.342% for the cycle pressure ratio of 40 to 220. Furthermore, fig.-3 shows the variations in mass liquefaction rate of various gases as described above with respect to cycle pressure ratio. It has been observed that methane has the highest liquefaction rate, which is varying from 0.02952kg/s to 0.1446kg/s for the cycle pressure ratio of 40 to 220, followed by argon, oxygen, air, nitrogen and fluorine, it has the minimum value of mass flow rate i.e., varies from 0.01222kg/s to 0.05655kg/s for the selected range of cycle pressure ratio of 40 to 220.

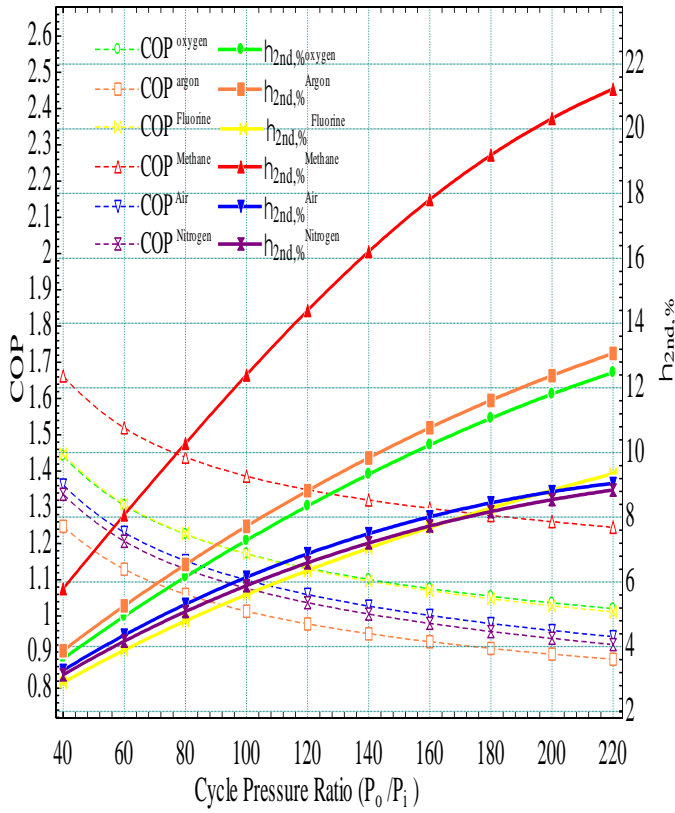


Figure 2: Variations in COP and second law efficiency with cycle pressure ratio

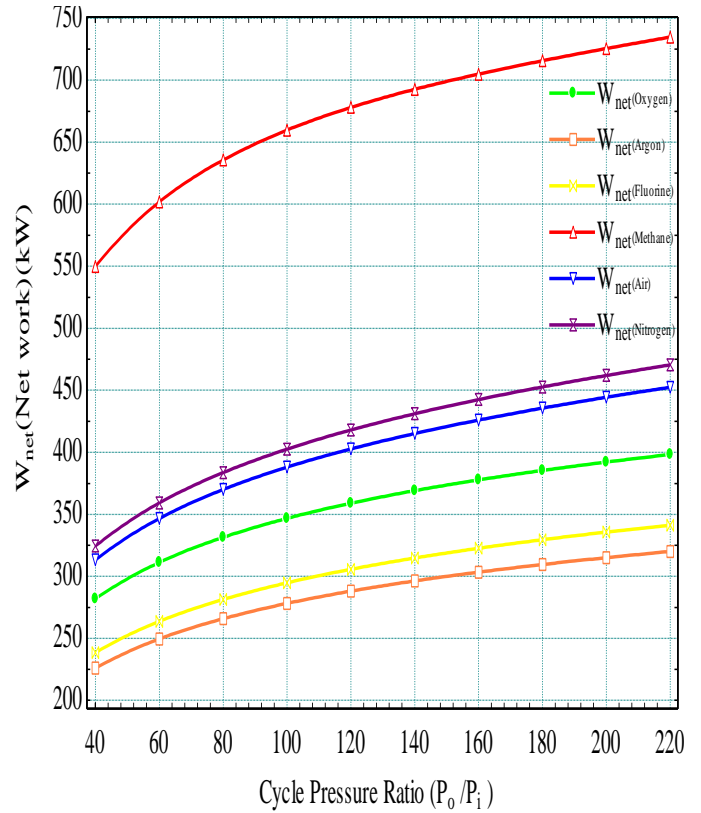


Figure 4: Variation in net work done with cycle pressure ratio

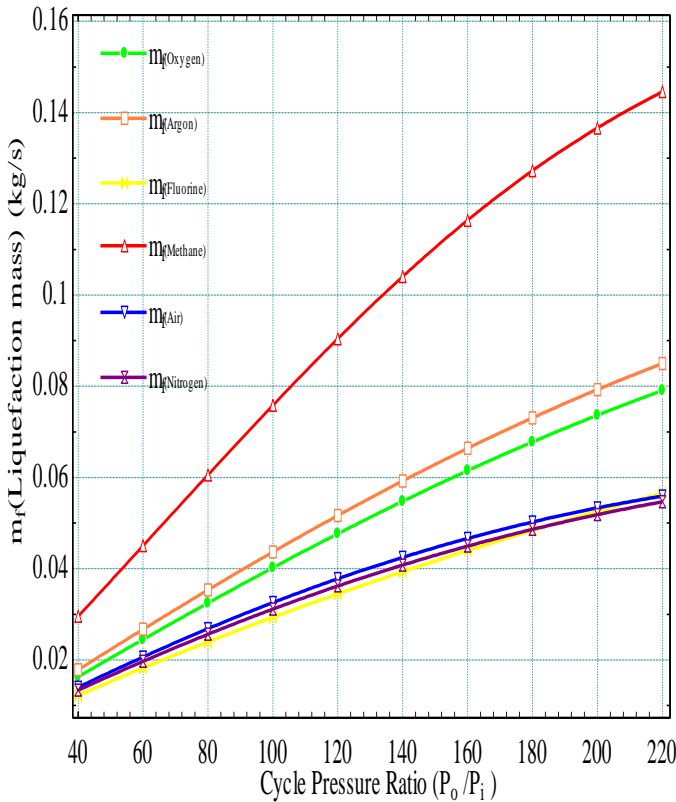


Figure 3: Variation in liquefaction mass flow with cycle pressure

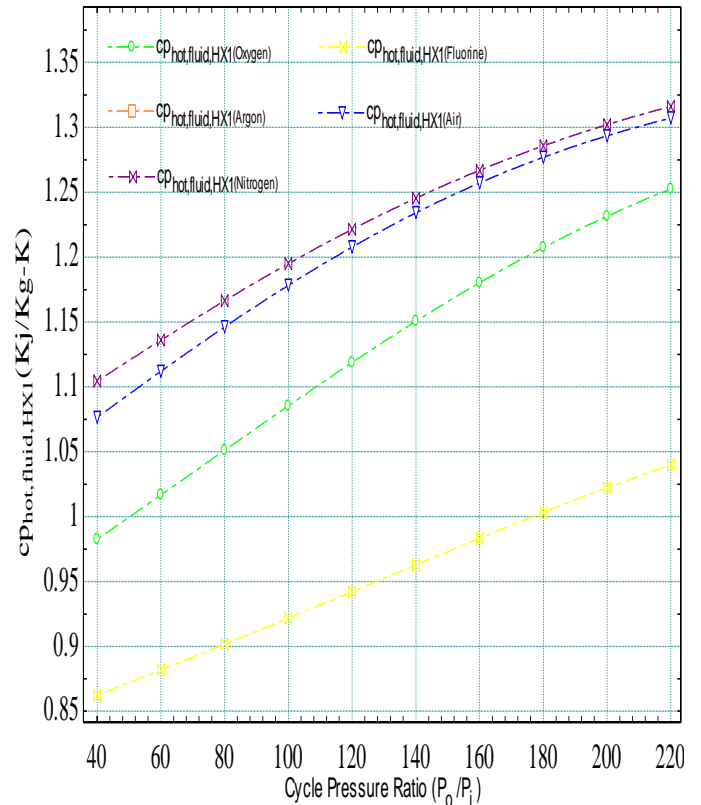


Figure 5: Variation in specific heat of hot fluid in HX1 with cycle pressure ratio

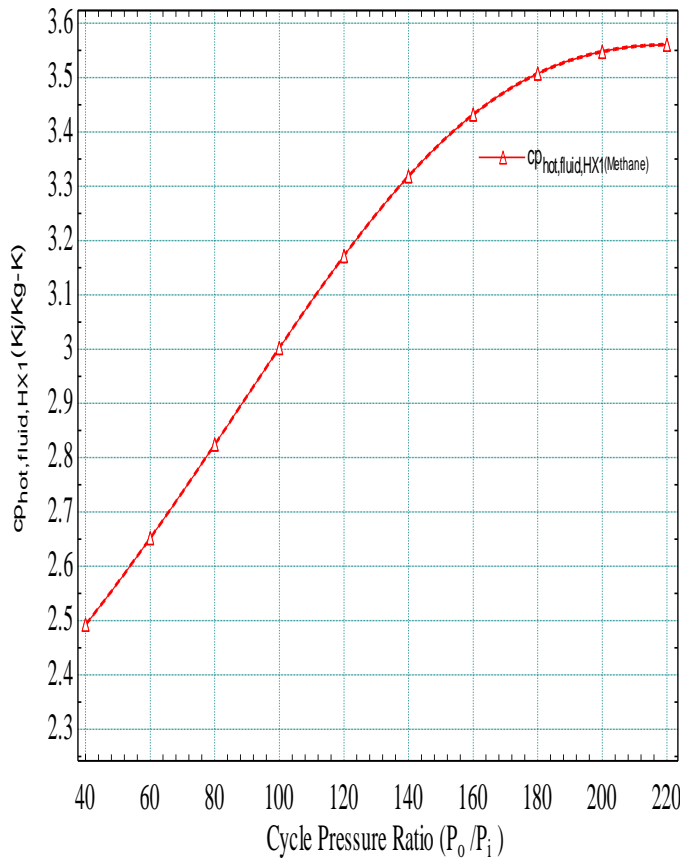


Figure 6: Variation in specific heat of hot fluid in HX1 with cycle pressure ratio

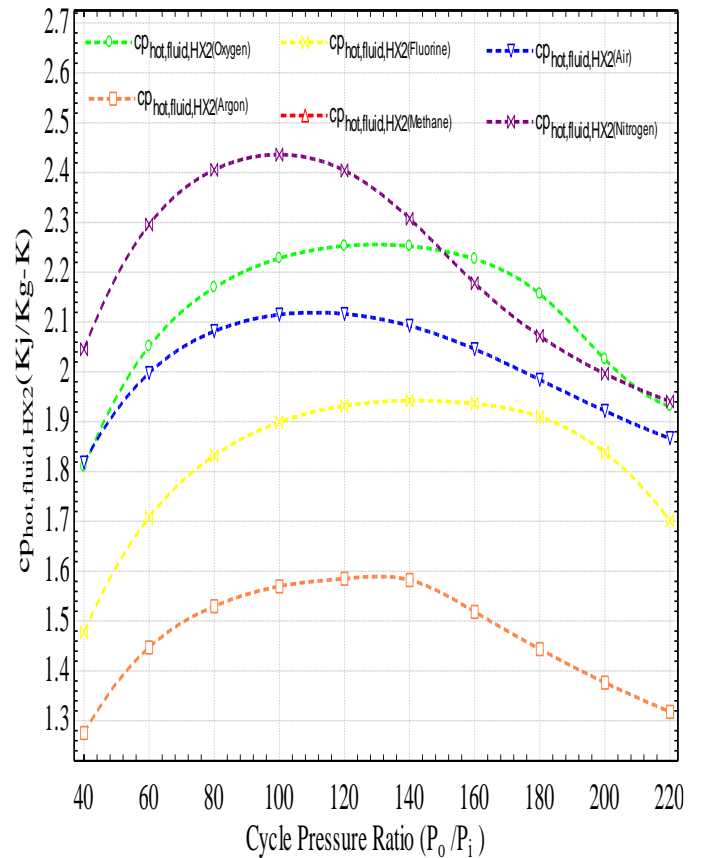


Figure 7: Variation in specific heat of hot fluid in HX2 with cycle pressure ratio

Fig.4 illustrates the variations in net work done with respect to cycle pressure ratio. It has been analyzed that methane has the highest value of net work done, which is increasing from 549.9kW to 734.8kW and argon has the least value of net workdone i.e., increasing from 226kW to 367.2kW for the selected range of cycle pressure ratio of 40 to 220. Fig.6 shows the variation in specific heat of hot fluid in HX1 with respect to cycle pressure ratio of 40 to 220. Fig.6 illustrates that methane has the highest value of specific heat for hot fluid, which is increasing from 2.493kJ/kg-K to 3.561kJ/kg-K. On the contrary side, fluorine has the least value of specific heat for hot fluid, which is enhanced from 0.8623kJ/kg-K to 1.04kJ/kg-K. Fig.7demonstrates the variations in specific heat of hot fluid in HX2 with respect to cycle pressure ratio of 40 to 220. It has been clearly understood from the fig.7 that nitrogen has the highest value of specific heat of hot fluid in HX2 among the other considered gases, which varies from 2.045 kJ/kg-K to 1.9411.04kJ/kg-K, and maximum value of specific heat of hot fluid is found to be 2.404 at cycle pressure ratio of 100, which is followed by oxygen, air, fluorine and argon, respectively.

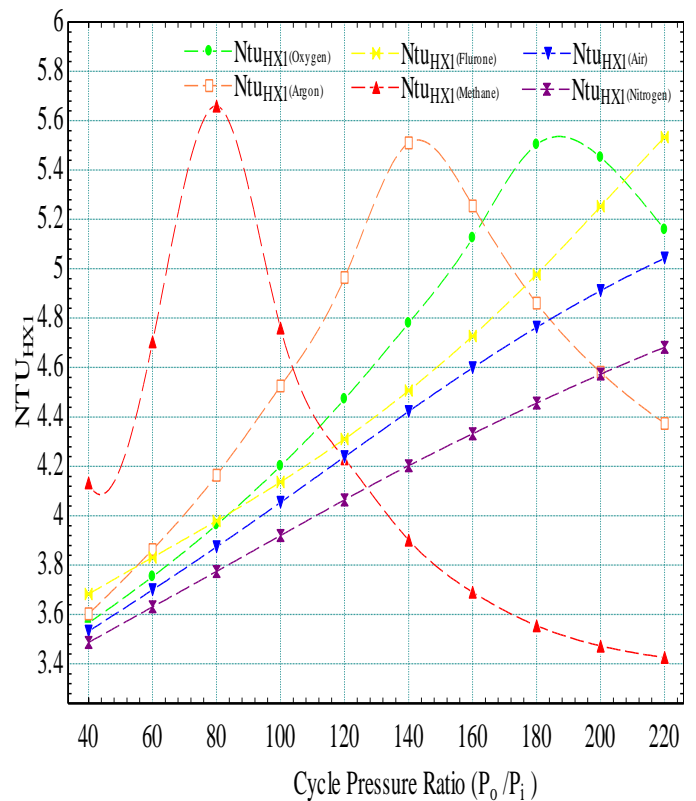


Figure 8: Variation in NTU in HX1 with cycle pressure ratio

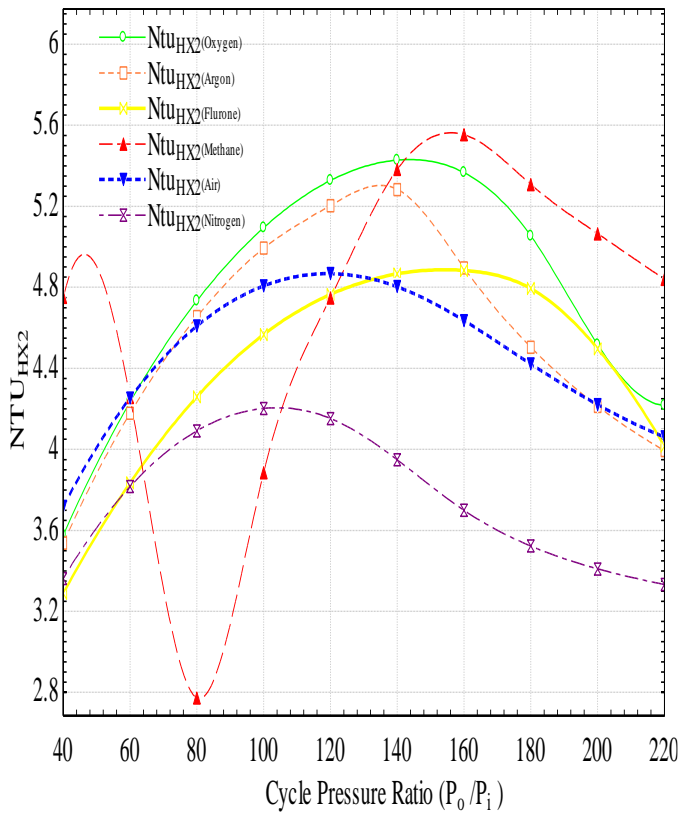


Figure 9: Variation in NTU in HX2 with cycle pressure ratio

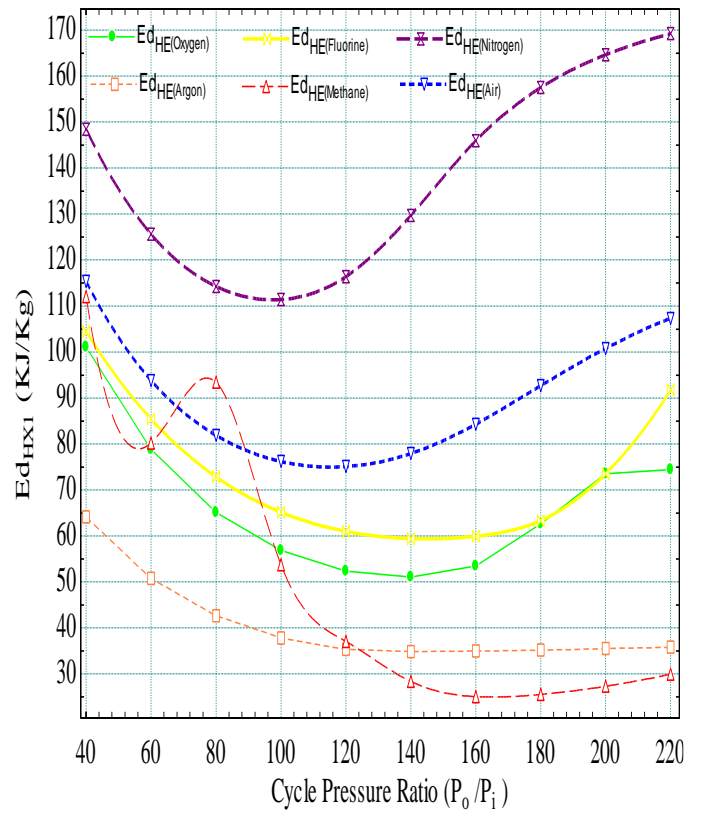


Figure 11: Variation in exergy destruction in HX1 with cycle pressure ratio

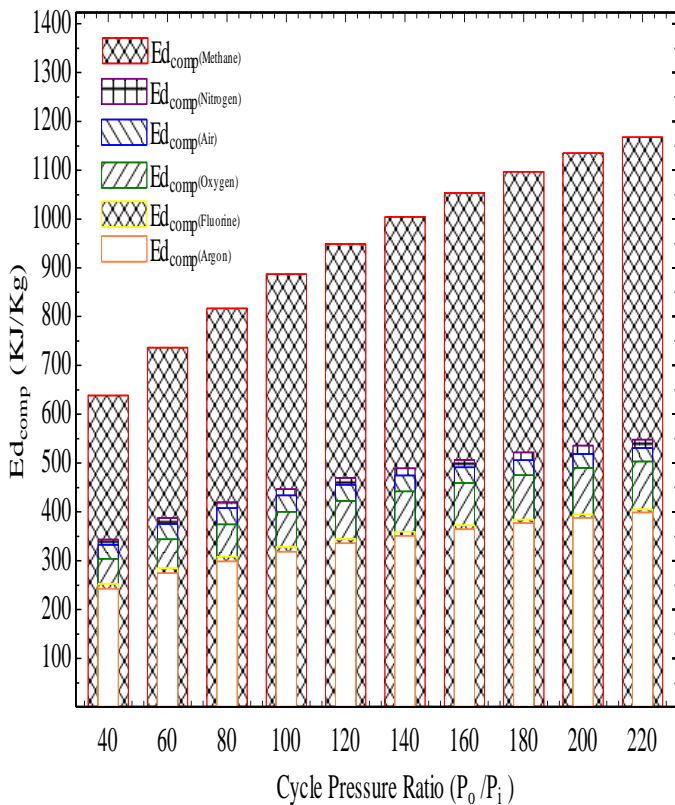


Figure 10: Variation of exergy destruction in compressor with cycle pressure ratio

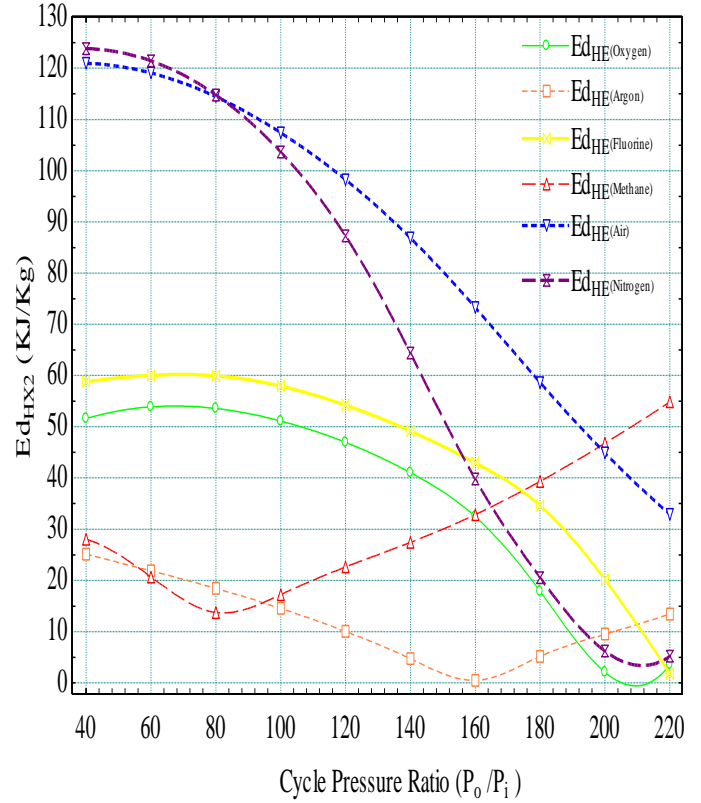


Figure 12: Variation in exergy destruction in HX2 with cycle pressure ratio

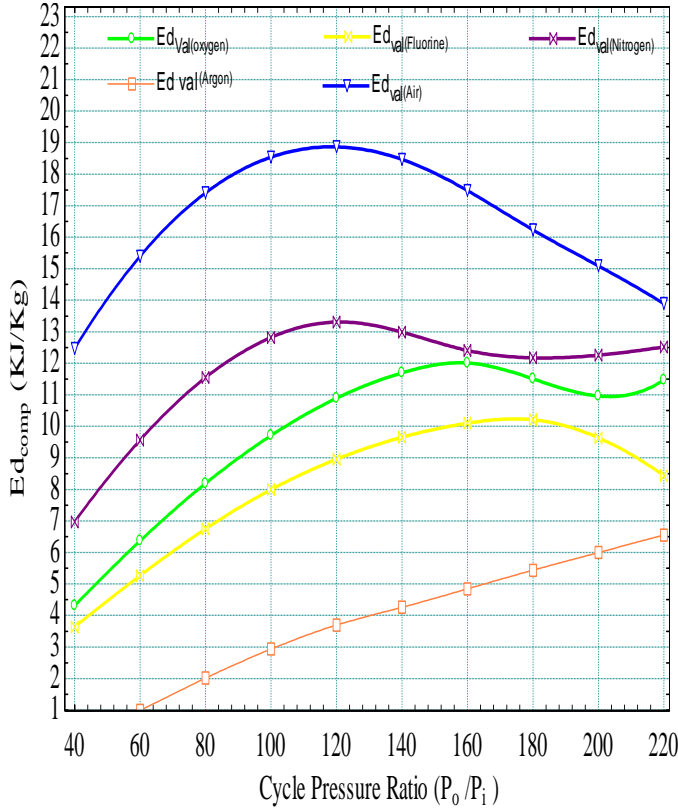


Figure 13: Variation in exergy destruction in compressor with cycle pressure ratio

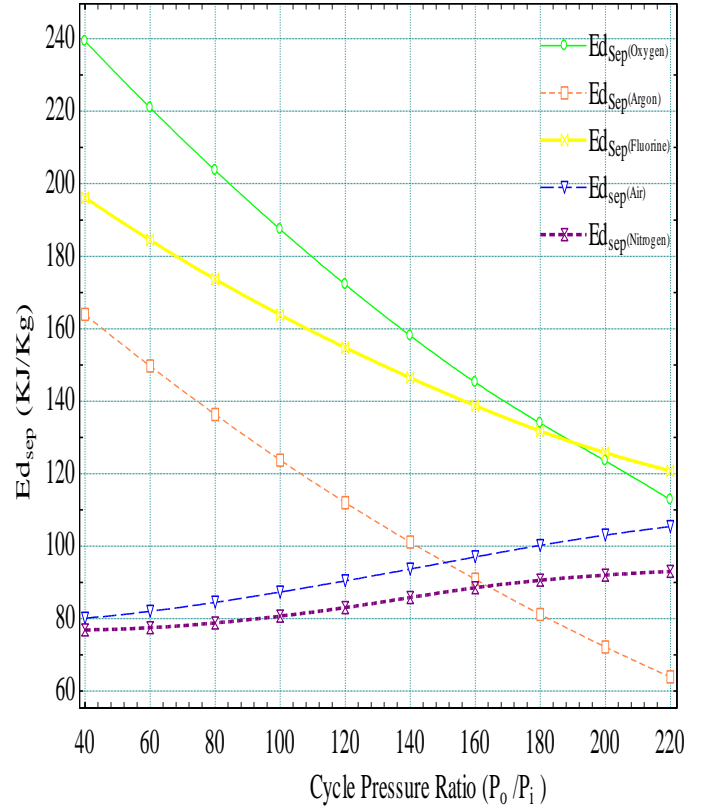


Figure 15: Variation in exergy destruction in separator with cycle pressure ratio

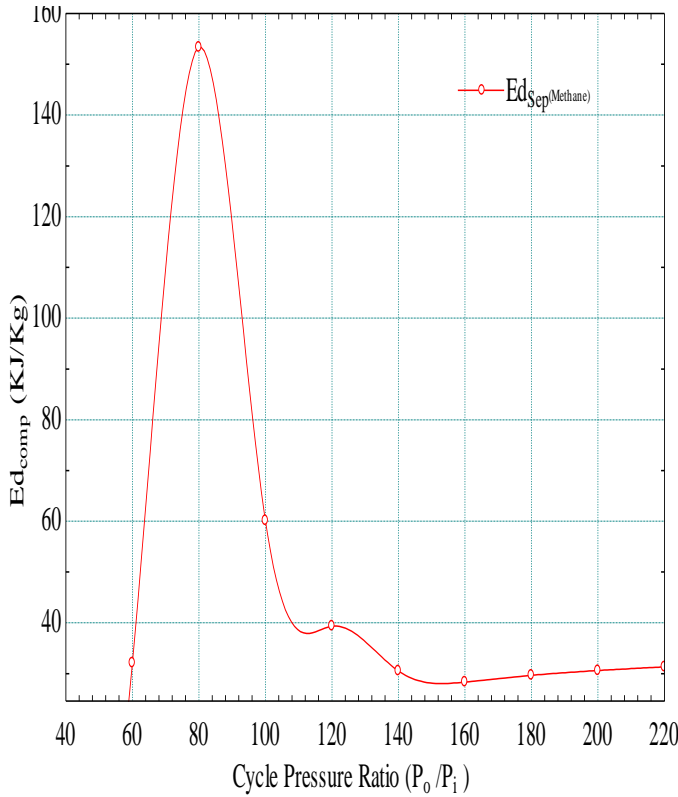


Figure 14: Variation in exergy destruction in compressor with cycle pressure ratio

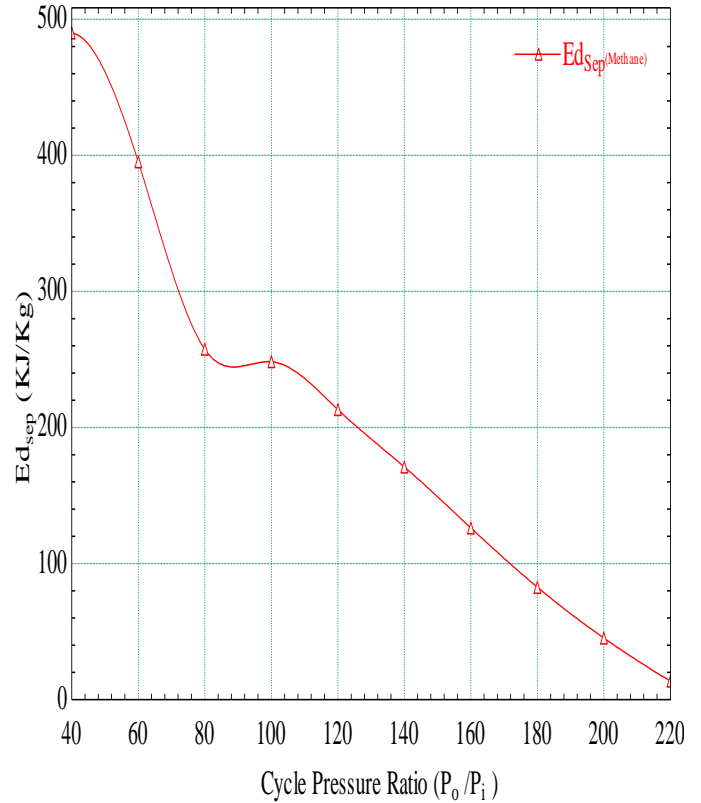


Figure 16: Variation in exergy destruction in separator with cycle pressure ratio

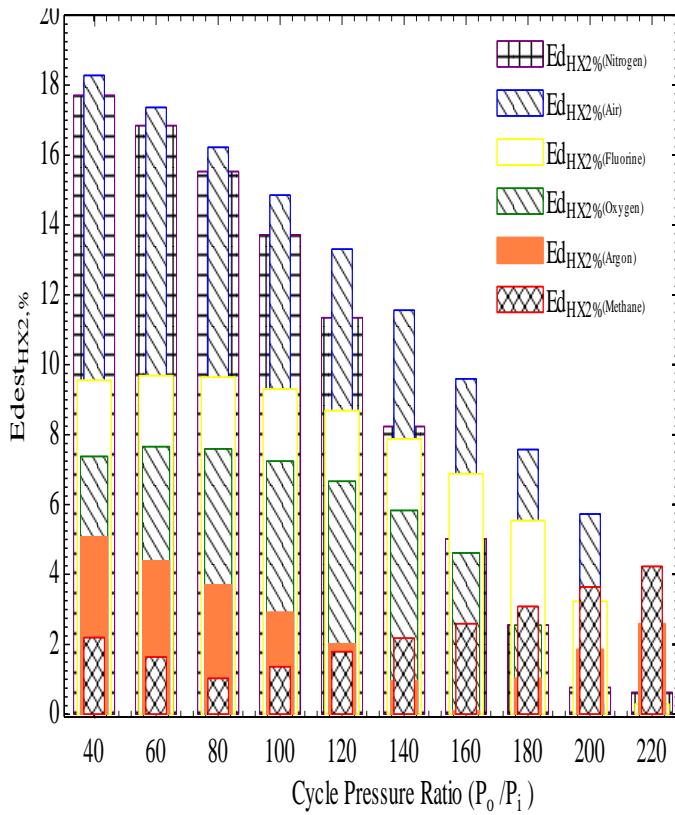


Figure 17: Variation in percentage exergy destruction in HX2 with cycle pressure ratio

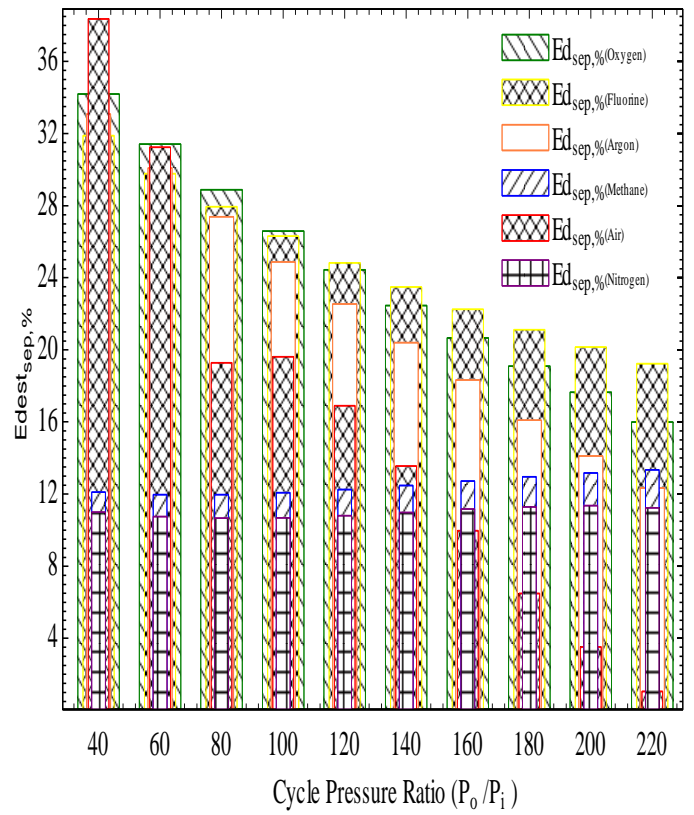


Figure 19: Variation in percentage exergy destruction with cycle pressure ratio

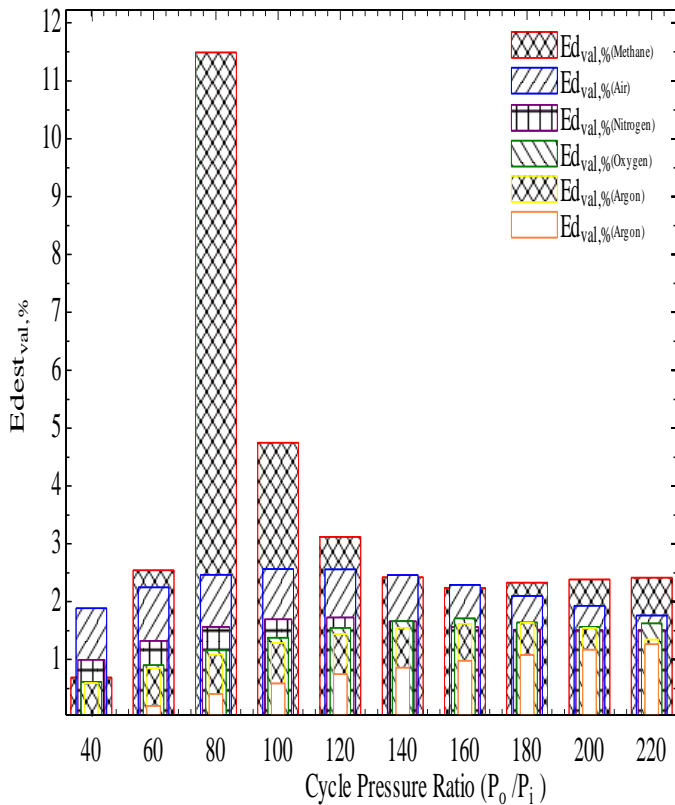


Figure 18: Variation in percentage exergy destruction in valve with cycle pressure ratio

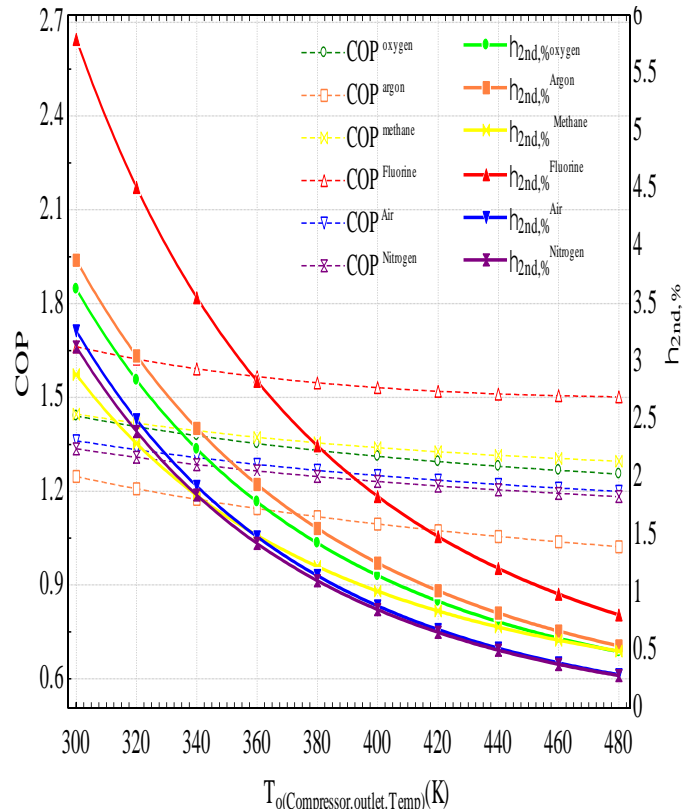


Figure 20: Variations in COP and second law efficiency with the compressor outlet temperature

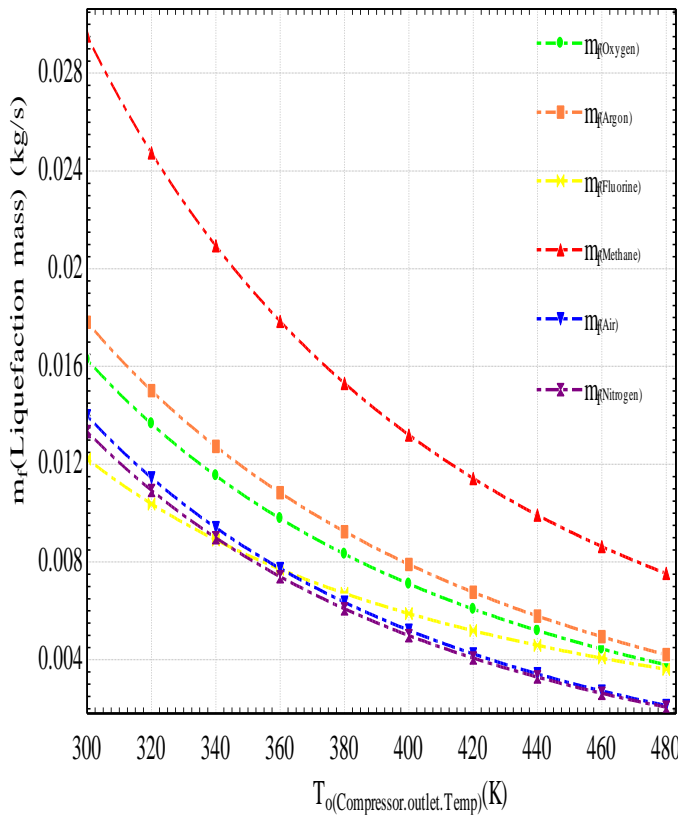


Figure 21: Variation in liquefaction mass flow with the compressor outlet temperature

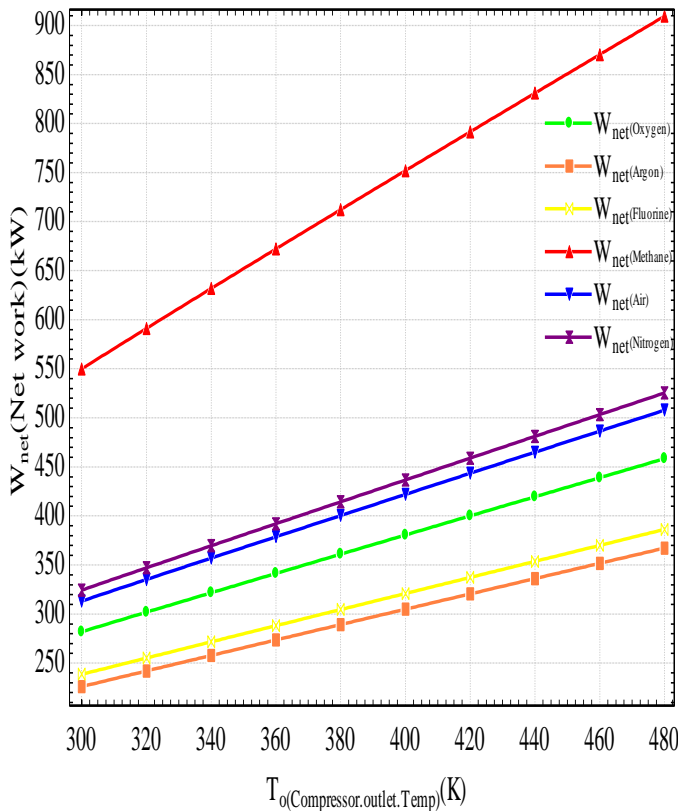


Figure 22: Variation in net work done with the compressor outlet temperature

Fig.8 shows the variations in NTU of HX1 with the cycle pressure ratio of 40 to 220. It has been seen that maximum incremental variations in NTU are found to be in methane i.e., 5.66 at cycle pressure of 80 and then its value suddenly decreases, which is followed by argon, oxygen, fluorine, air, and nitrogen shows the continuous increasing behaviour, i.e., varies from 3.487 to 4.682. On the other hand, fig.9 shows the variations in NTU of HX2 with the cycle pressure ratio of 40 to 220. It has been seen that methane shows decrement in NTU value initially then suddenly increase and goes up to the maximum point i.e. 5.553 at around 160. While all other gases shows almost the same type of behaviour i.e., increase first and then decrease. Oxygen shows the better results for NTU in HX2 i.e. changes from 3.577 to 4.217 followed by argon, air, fluorine, and nitrogen shows the least value i.e., varies from 3.362 to 3.333. Fig.10 illustrates the exergy destruction rate of compressor with respect to cycle pressure ratio of 40 to 220. It has been clearly understood from the graphs that exergy destruction rate is continuously increasing, and methane has the highest value of exergy destruction rate among the other gases and it is increasing from 638.3kJ/kg to 1168kJ/kg. Alternatively, argon has the least value of exergy destruction rate of compressor i.e. increases from 242.4kJ/kg to 371.5kJ/kg.

Fig.11 demonstrates the exergy destruction rate of HX1 with respect to cycle pressure ratio of 40 to 220. It has been found that nitrogen shows the highest exergy destruction rate in HX1, i.e., 148.4kJ/kg to 169.2kJ/kg. On the other side, fig.12 illustrates that nitrogen and air both show the highest rate of exergy destruction in HX2 among the other gases, i.e., 123.8kJ/kg and 120.9kJ/kg, respectively. Fig.13 and fig.14 shows the exergy destruction rate of valve with respect to cycle pressure ratio of 40 to 220. Methane shows the highest value of exergy destruction among the other gases, and it attains maximum value i.e. 153.4kJ/kg at cycle pressure ratio of 80 as shown in fig.14. While argon having the least value of exergy destruction rate, i.e., increases from 0.0399kJ/kg to 6.552kJ/kg as shown in Fig.13.

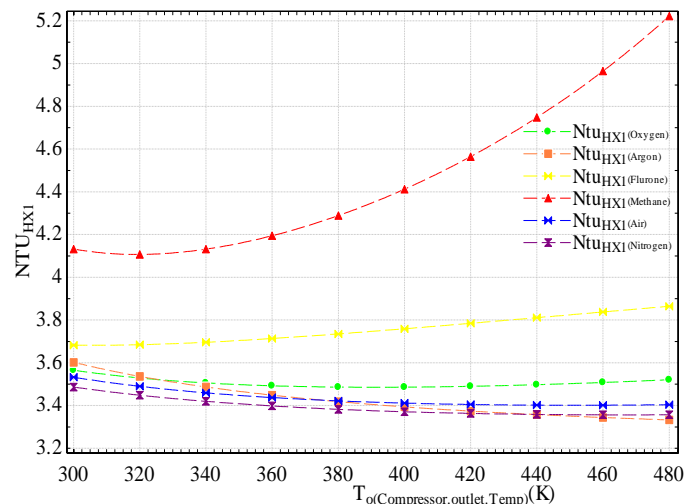


Figure 23: Variation in NTU in HX1 with compressor outlet temperature

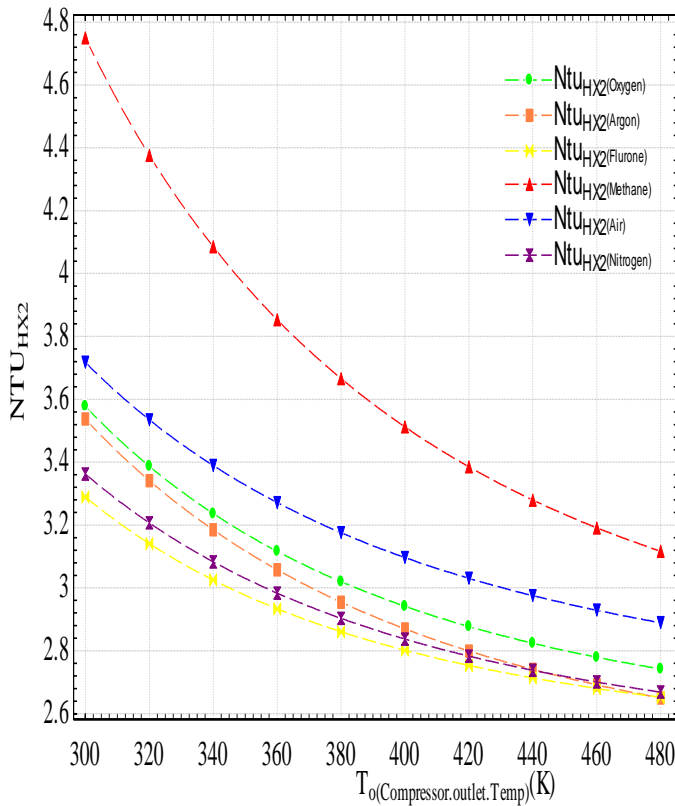


Figure 24: Variation in NTU in HX2 with compressor outlet temperature

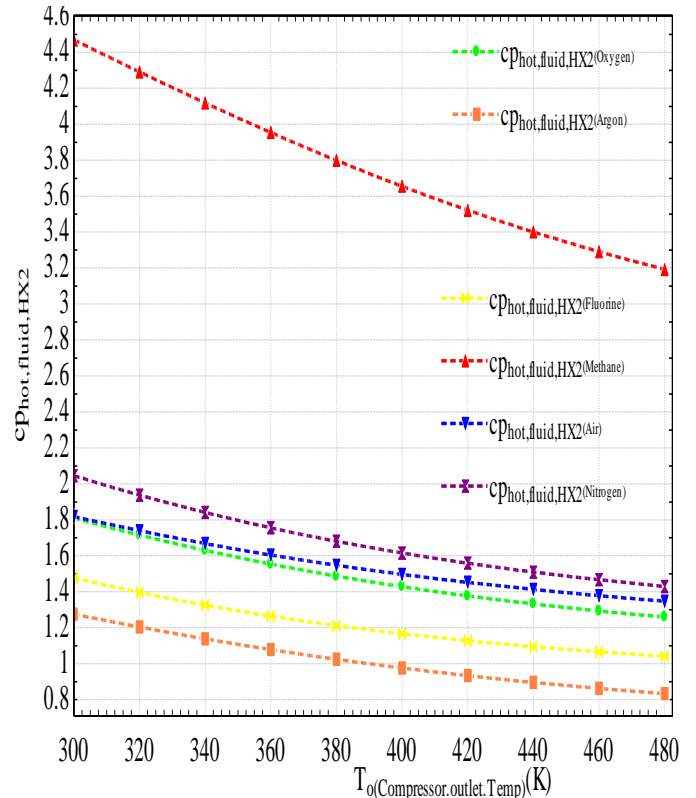


Figure 26: Variation in specific heat of hot fluid in HX2 with the compressor outlet temperature

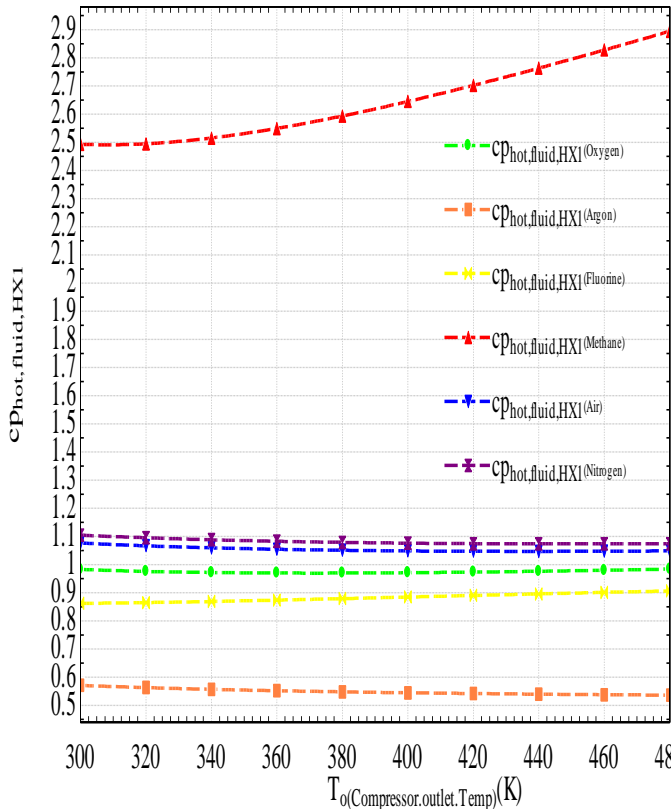


Figure 25: Variation in specific heat of hot fluid in HX1 with the compressor outlet temperature

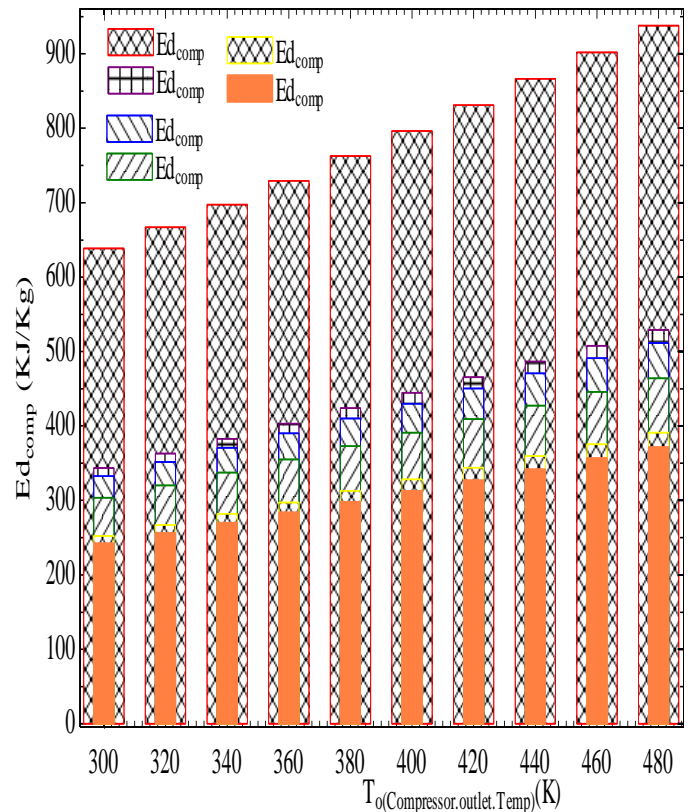


Figure 27: Variation in exergy destruction in compressor with the compressor outlet temperature

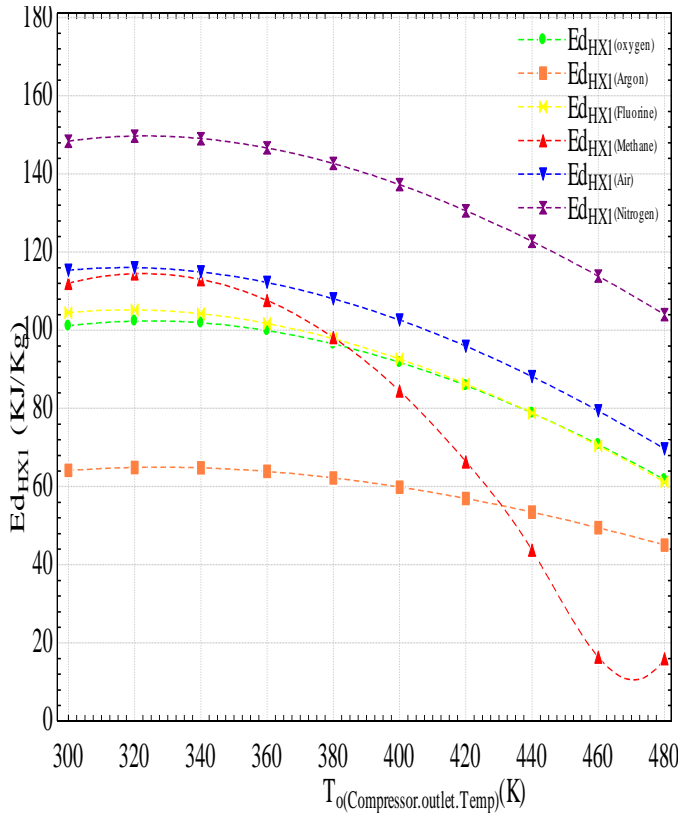


Figure 28: Variation in exergy destruction in HX1 with the compressor outlet temperature

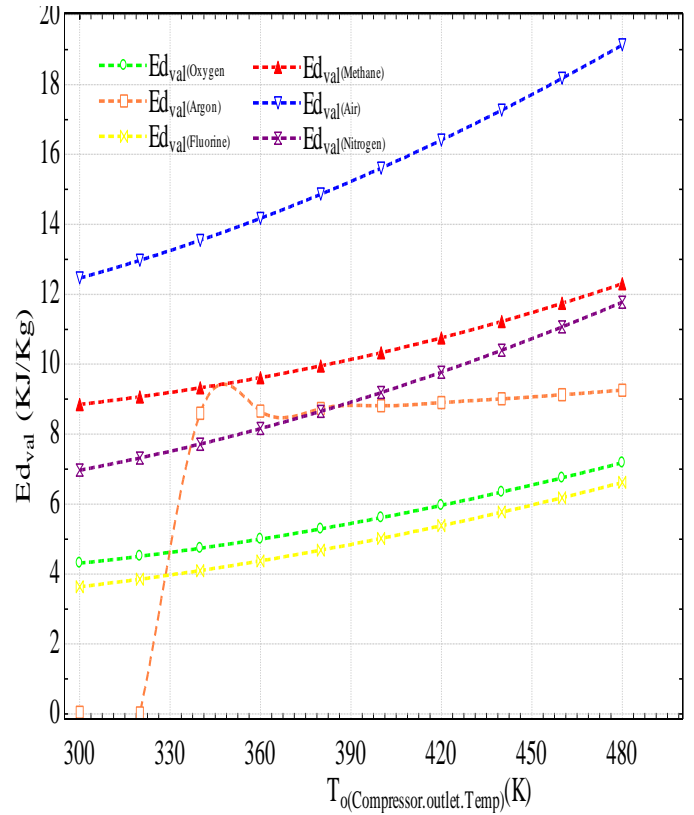


Figure 30: Variation in exergy destruction in VALVE with the compressor outlet temperature

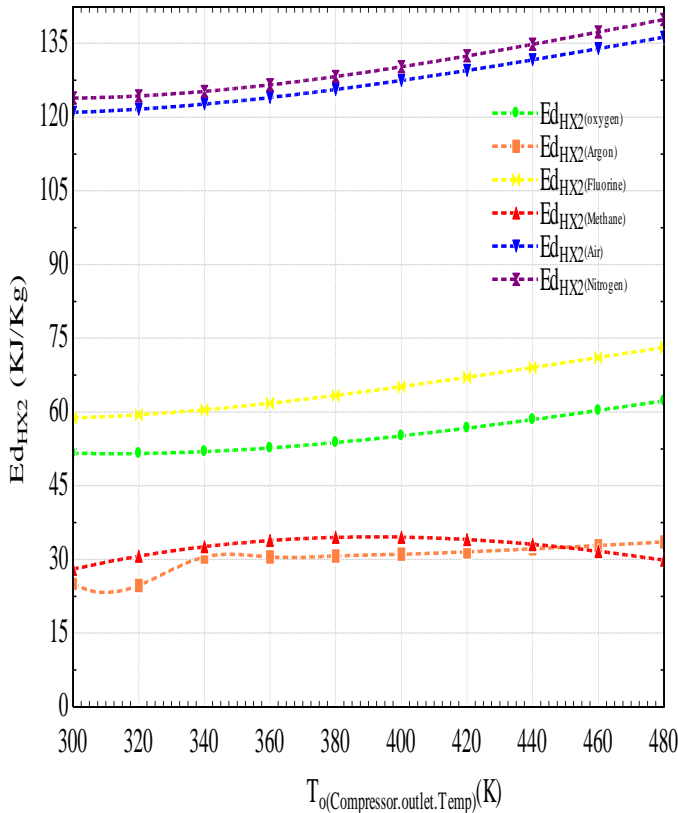


Figure 29: Variation in exergy destruction in HX2 with the compressor outlet temperature

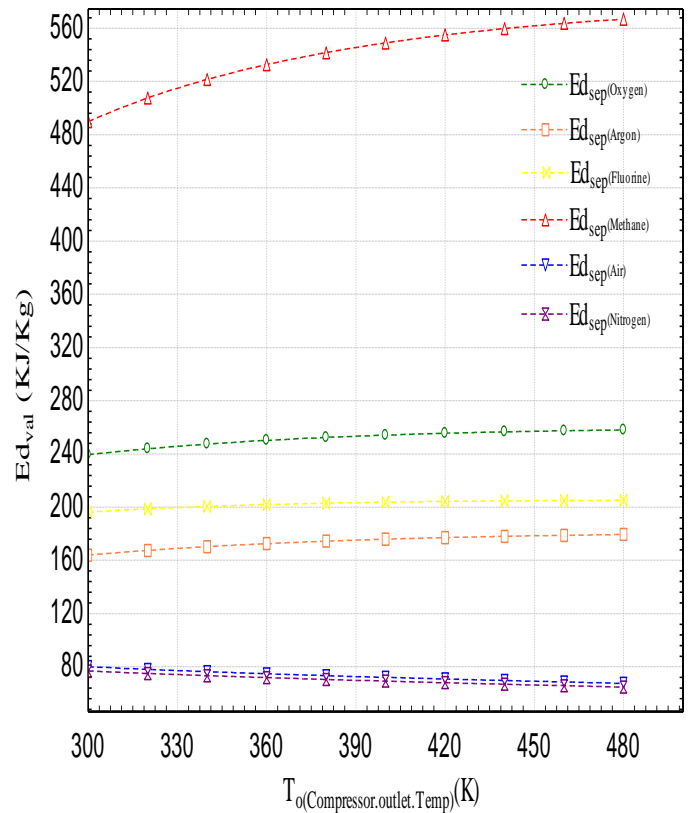


Figure 31: Variation in exergy destruction in valve with the compressor outlet temperature

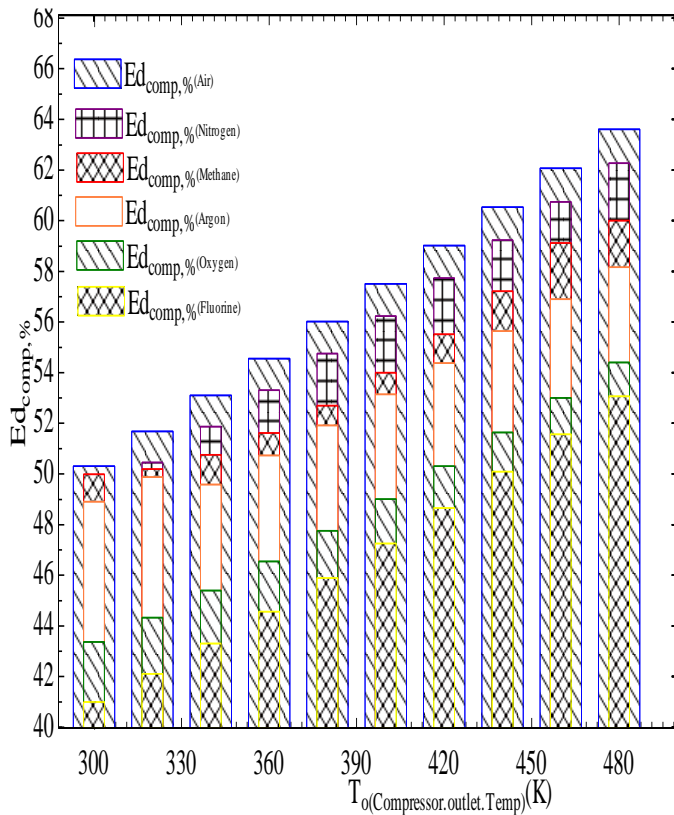


Figure 32: Variation in percentage exergy destruction in ompressor with the compressor outlet temperature

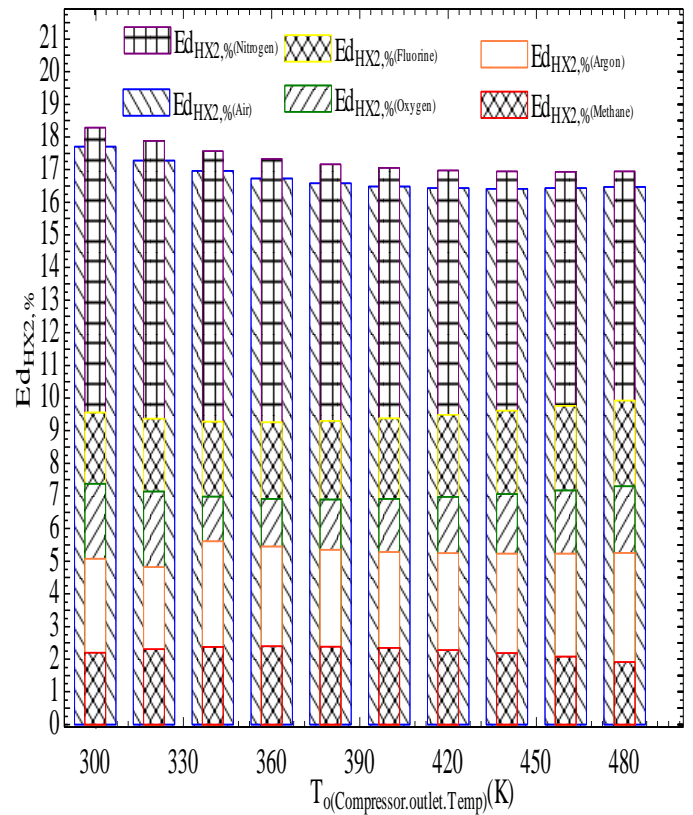


Figure 34: Variation in percentage exergy destruction in HX2 with the compressor outlet temperature

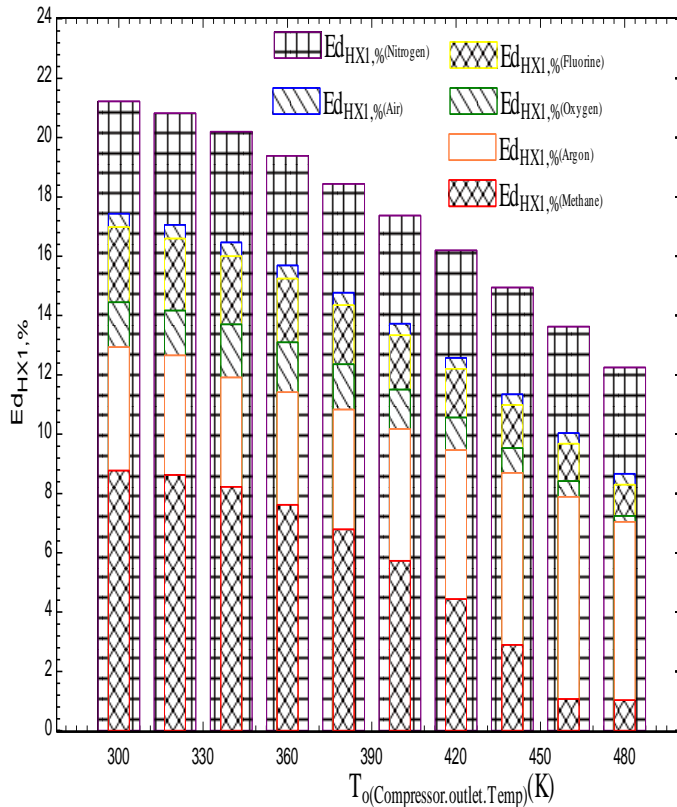


Figure 33: Variation in percentage exergy destruction in HX1 with the compressor outlet temperature

Fig.13 and fig.15 shows the exergy destruction rate of separator with the cycle pressure ratio of 40 to 220. It has been seen that methane has the highest rate of exergy destruction in separator, which decreases from 163.9kJ/kg to 63.86kJ/kg followed by oxygen, fluorine and argon. While air and nitrogen having the slightly increasing trend of exergy destruction rate with the lowest value in separator among other gases.

Fig.16 illustrates the percentage exergy destruction in compressor with cycle pressure ratio of 40 to 220. It has been observed that methane has the highest percentage exergy destruction rate and nitrogen having the least value of exergy destruction rate, which is around 49.98% to 90% and 49.09% to 66.19%, respectively. On the other hand, fig.17 demonstrates the percentage exergy destruction in HX1 with the cycle pressure ratio as described above. Nitrogen having the highest and methane has the lowest percentage of exergy destruction rate, i.e., around 21.22% to 20.44% and 8.772% to 2.307%, respectively. Furthermore, the variations in percentage exergy destruction in the HX2 with cycle pressure ratio of 40 to 220 as shown in Fig.18. It has been noticed that air has the highest percentage of exergy destruction, which is changing from 18.28% to 4.163%. While methane and argon have the minimum percentage of exergy destruction rate, i.e., varies from 2.193% to 4.228% and 5.074% to 2.588%. Fig.19 shows that methane has the highest variations in percentage of exergy destruction rate in valve, which is found to be 11.49% at cycle pressure ratio of 80. Moreover, fig.20 illustrates that fluorine and oxygen have comparatively highest percentage of

exergy destruction rate in separator among the other gases, which varies from 31.88% to 19.23% and 34.2% to 15.98%, respectively. Also, fig.21 shows the variations in the COP and second law efficiency with respect to compressor outlet temperature of 300K to 480K. It has been noticed that fluorine shows the highest value of COP and second law efficiency i.e., 1.447 to 1.296 and 2.889% to 0.4946%, respectively. Fig.22 shows the variations in the liquefaction mass flow rate with respect to compressor outlet temperature of 300K to 480K. It has been observed that methane has the highest value of liquefaction mass flow rate among the other gases i.e., 0.02952kg to 0.00753kg. Fig.23 demonstrates the variations in net work done with respect to compressor outlet temperature of 300K to 480K. It has been seen that methane shows the highest value of net work done among the other gases, which is increasing from 549.9kW to 909.4kW. Alternatively, argon having the minimum value of net workdone, i.e., increasing from 226kW to 367.2kW. Fig.24 shows the variations in NTU of HX1 with the compressor outlet temperature. The trend of this graph is first slightly decreasing and then increasing suddenly. It has been seen that methane has the highest NTU in HX1 among the other gases, i.e., 5.222 at 480K. On the other hand, Fig.25 illustrates the variations in NTU of HX2 with the compressor outlet temperature. It has been analyzed that methane has the maximum NTU in HX2, i.e., 4.75 at 300K and, graph is continuously decreasing. Fig.26 demonstrates the variations in specific heat of the hot fluid in HX1 and it has been observed that methane has the highest value of specific heat among the other gases, which is increases from 2.493kJ/kg-K to 2.895kJ/kg-K. While all other gases show slightly decreasing trend of specific heat of hot fluid in HX1. Alternatively, Fig.26 shows the variations in specific heat of hot fluid in HX2 with compressor outlet temperature. Again methane has the highest value of specific heat of hot fluid among other gases, i.e., 4.468 kJ/kg-K at 300K, and it is decreasing continuously. Fig.26 indicates the variations in exergy destruction rate variations with the compressor outlet temperature. It has been analyzed that methane has the highest rate of exergy destruction rate among the others i.e. 937.7kW at 480K. Fig. 33 shows the variations in exergy destruction rate in HX1 with the compressor outlet temperature and it has been observed that nitrogen has the highest rate of exergy destruction rate i.e. 148.4kW at 300K. Fig.27 shows the variations in exergy destruction rate in HX2 with the compressor outlet temperature and it has been observed that nitrogen has the highest rate of exergy destruction rate i.e., 139.9kW at 480K. Fig.28 shows the variations in exergy destruction rate in valve with the compressor outlet temperature and it has been observed that air has the again highest rate of exergy destruction rate i.e., 19.13kW at 300K. Fig.29 shows the variations in exergy destruction rate in separator with the compressor outlet temperature and it has been observed that methane has the highest rate of exergy destruction rate i.e., 566.8kW at 480K. In addition, Fig.30 shows the variations in percentage exergy destruction rate in compressor with the compressor outlet temperature and it has been observed that air has the highest rate of exergy destruction rate i.e., 63.61% at 300K.

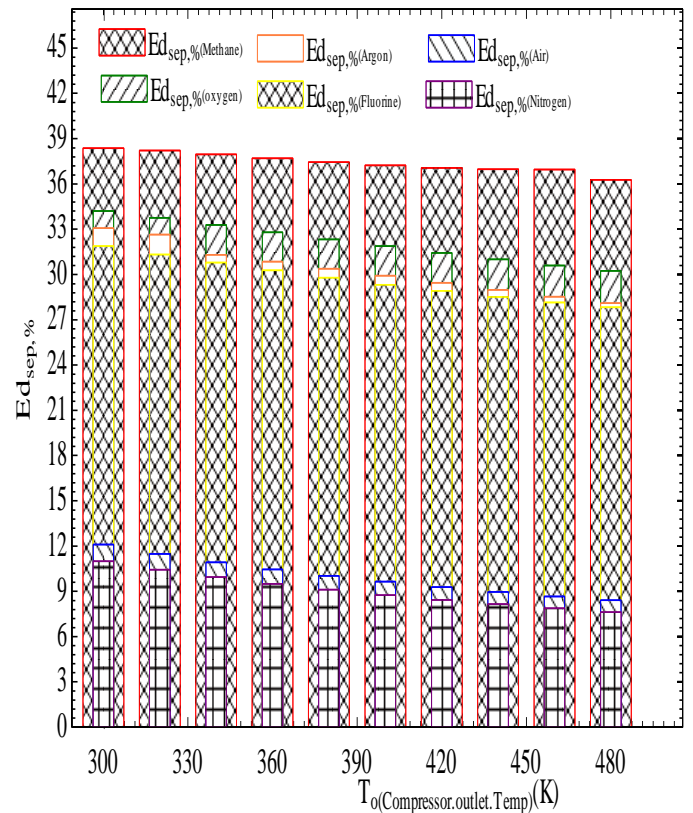


Figure 35: Variation in in exergy destruction in separator with the compressor outlet temperature

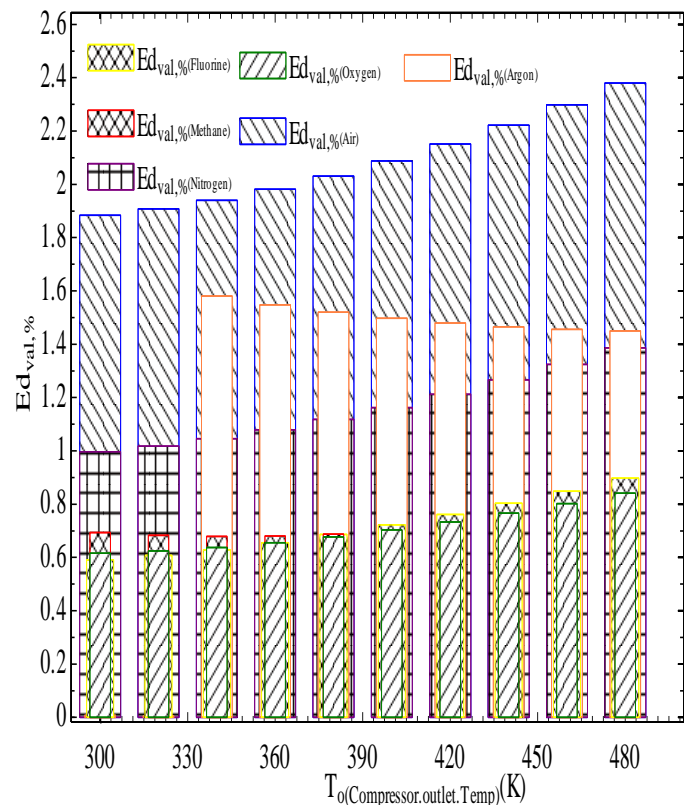


Figure 36: Variation in in exergy destruction in valve with the compressor outlet temperature

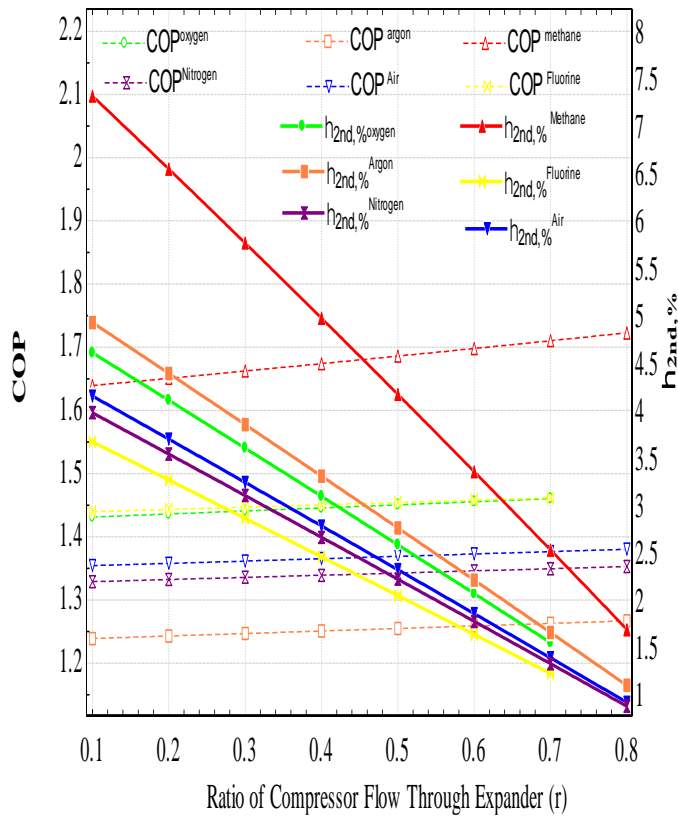


Figure 37: Variation in COP and second law efficiency with the ratio of compressor flow through expander

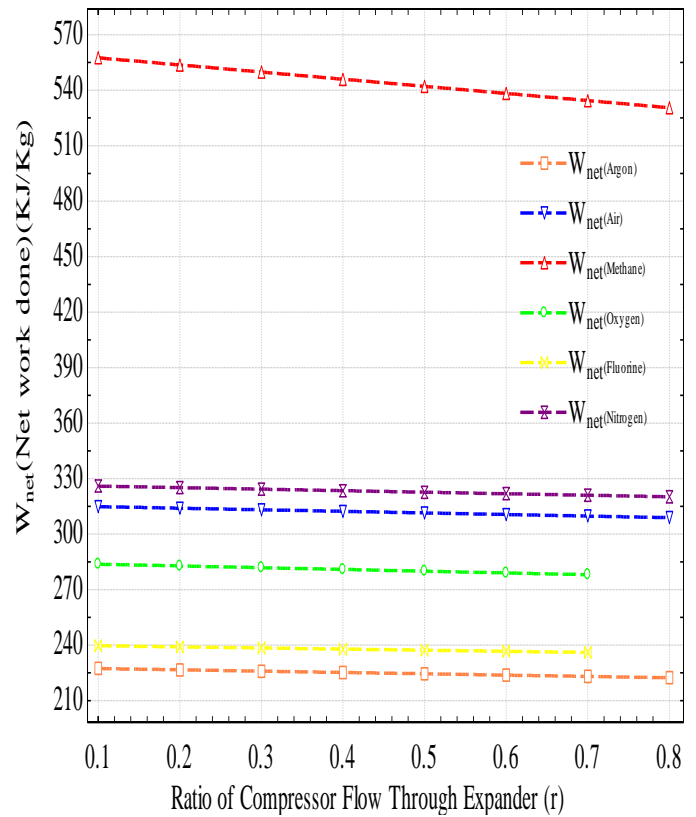


Figure 39: Variation in net work done with the ratio of compressor flow through expander

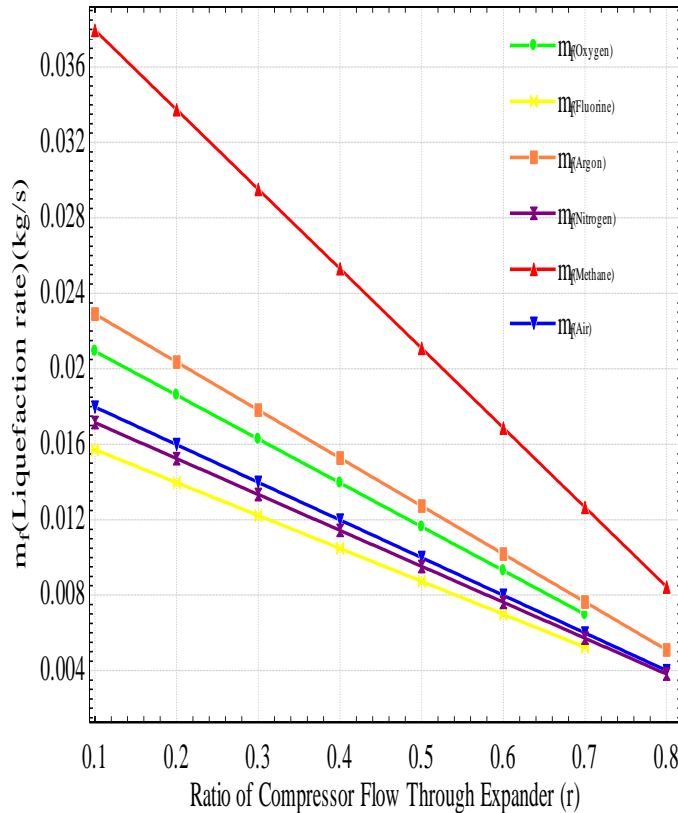


Figure 38: Variation in liquefaction mass flow with the ratio of compressor flow through expander

Fig.30 shows the variations in percentage exergy destruction rate in HX1 with the compressor outlet temperature and it has been observed that nitrogen has the again highest rate of exergy destruction rate i.e., 21.22% at 300K. Fig.31 illustrates the variations in percentage exergy destruction rate in HX2 with the compressor outlet temperature and it has been observed that nitrogen has the highest rate of exergy destruction rate i.e., 17.71% at 300K. Fig.32 illustrates the variations in percentage exergy destruction rate in separator with the compressor outlet temperature and it has been observed that methane has the highest rate of exergy destruction rate i.e., 38.36% at 300K. Fig.33 indicates the variations in percentage exergy destruction rate in valve with the compressor outlet temperature and it has been observed that air has the highest rate of exergy destruction rate i.e., 19.13% at 480K. Fig.34 illustrates variations in COP and second law efficiency with respect to ratio of compressor flow through expander. It has been seen that methane has the highest COP and second law efficiency among other gases i.e., 1.723 at 0.8 and 7.344% at 0.1, respectively. Fig.35 shows the variations in mass liquefaction rate with respect to ratio of compressor flow ratio and it has been analyzed that methane has the highest mass liquefaction rate i.e. 0.03795 at 0.1 and it is decreasing continuously, i.e. 0.008433 at 0.8 followed by other considered gases. Last but not the least, fig. 39 shows the variations in net work done with respect to the ratio of compressor flow ratio. It has been observed that methane has the highest net work done among other gases, which is exactly 557.6kW at 0.1 compressor flow ratio and argon shows the least value of net

work done i.e. 227.4kW at the same compressor flow ratio of 0.1.

5. Conclusions

Exergy analysis of Haylent system and its component with different gasses help in determine the best thermodynamic performance parameters for each given gas liquefaction process. Various performance parameters have been studied with increasing pressure ratio. Following points are concluded from the present investigation

- (1) COP and Second law efficiency of system is degrading at high pressure for all gasses.
- (2) The optimum performance pressure ratio range for system is 140-160 bar.
- (3) Among all six gases methane gas liquefaction process required more attention.
- (4) Gas of the liquefaction is very important factor in determine the most exergy destructions causing component of Haylent system.

References

- [1] R. Agrawal, D.W. Woodward, Efficient cryogenic nitrogen generators: An exergy analysis, Gas Separation & Purification, Volume 5, Issue 3, September 1991, Pages 139-150
- [2] Yasuki Kansha, Akira Kishimoto, Tsuguhiko Nakagawa, Atsushi Tsutsumi, A novel cryogenic air separation process based on self-heat recuperation, Separation and Purification Technology, Volume 77, Issue 3, 4 March 2011, Pages 389-396
- [3] Gadhiraaju Venkatarathnam , “Simulation of cryogenic processes” , Cryogenic Mixed Refrigerant Processes ,International Cryogenics Monograph Series 2008, , Pages 51-63
- [4] R.L. Cornelissen, G.G. Hirs, Exergy analysis of cryogenic air separation, Energy Conversion and Management, Volume 39, Issues 16–18, November–December 1998, Pages 1821-1826,.